

POSITION DETERMINATION OF RESIDENT SPACE OBJECTS VIA TRIANGULATION WITH TWO PASSIVE-OPTICAL STARING SYSTEMS

Ranga Rosok⁽¹⁾, Nikolai Hoffmann⁽¹⁾, Moritz Vogel⁽¹⁾, Felicitas Niebler⁽¹⁾, Nils Bartels⁽¹⁾, and Paul Wagner⁽²⁾

⁽¹⁾Institute for Technical Physics, German Aerospace Center (DLR), Stuttgart, Germany, Email: ranga.rosok@dlr.de

⁽²⁾Institute of Communications and Navigation, German Aerospace Center (DLR), Oberpfaffenhofen, Germany

ABSTRACT

The number of space objects orbiting the Earth is rapidly increasing. An opportunity to detect and measure the position of space objects are passive optical staring systems, e.g. our system called APPARILLO. While staring systems are capable of measuring highly accurate equatorial coordinates of space objects via an astrometric calibration, they do not provide information on their altitude unless the space object is assumed to fly on a circular orbit. In this work we discuss an approach in which the altitude of a space object is measured via triangulation (simultaneous observation with two staring systems placed at different positions on Earth). Based on theoretical calculations, we estimate that the triangulation with two staring systems can provide the altitude of a typical space object in a low Earth orbit with an accuracy as low as 200 m. This is two orders of magnitude better compared to a simple circular orbit approximation that can be used for a single staring system.

Keywords: Passive Optical Staring; Bi-Static Measurement; Initial Space Debris Detection; Low Earth Orbit; Space Situational Awareness.

1. INTRODUCTION

The number of space objects orbiting our Earth is rising rapidly. This leads to more and more frequent convergences, which pose a potential threat for the two as well as for other satellites. To ensure safety in space for current and future missions, continuous monitoring of the entire space is essential. Some common methods are listed below.

Radar sensors [1] can scan space day and night, regardless of the weather and the lighting. A disadvantage of such a system is the high cost involved in building and operating it.

Satellite laser ranging systems [2] deliver extremely precise orbit information of individual satellites. However, they need orbit information in advance, which is for example provided by a radar system.

Passive optical staring systems offer another possibility

to provide this orbit information on a large scale. They benefit from their low cost and their flexibility.

We are developing a solution for an accurate three-dimensional passive optical tracking system for low Earth orbit (LEO) objects, the APPARILLOs [3] (abbrev. Autonomous Passive-Optical Staring of LEO Flying Objects).

An APPARILLO, Fig. 1, is based on a sensitive camera



Figure 1. Single APPARILLO staring system located at the DLR in Stuttgart.

that records images of the sky during twilight and nighttime periods. Secondary sensors like a weather sensor, a light sensor and a GPS module complement the image taking process. The whole system is controlled by a local computer which runs the software OOOS [4] (Orbital Objects Observation Software). This software controls everything beginning from the evaluation of the observation condition, over the image acquisition, the image analysis [5] up to the processed data upload.

Each system itself is highly modular, which offers great flexibility in terms of applications and equipment. For example, the lens can easily be switched to a longer/shorter focal length to detect smaller/more targets, the camera can be swapped out for another model specified for dif-

ferent wavelengths or with greater resolution. That flexibility not only makes it a versatile system that can be adapted to the current needs, it also enables easy and inexpensive repairs and upgrades to react to the latest technical developments.

In previous work [6] it is shown that one APPARILLO is able to detect objects down to a diameter of 25 cm in LEO. The measurement is accurate up to a 700 m along track and for the cross-track position even up to 30 m. A single APPARILLO can detect a large number of objects at a time. Up to 160 LEO objects per hour have been detected in previous observation campaigns, two thirds of which have been identified and the other third categorised as a "new" discovery. These "new" detections could not be correlated with the publicly available space track TLE catalogs [7].

The coordinates of the detected objects from one APPARILLO are given in equatorial coordinates. These are two dimensional coordinates, which are used to locate for example stars and satellite in the sky. Due to the working principle of a camera, information of the third dimension cannot be measured using a single system. With the help of two systems and triangulation, the orbital altitude of a satellite and thus the third spatial dimension can be determined [8, 9]. The goal of this work is to find an optimal configuration consisting of the spacing, the observation direction and the hardware of these systems in order to determine the altitude as precisely as possible.

2. CIRCULAR ORBITS

The first and simplest step in implementing an altitude measurement is to estimate its value based on the measured orbit parameters. In this case the velocity $|\dot{\mathbf{r}}|$ is required. The assumption needed to perform this approximation is that the Resident Space Object (RSO) is on a circular orbit. An object (at the position \mathbf{r}) that moves in the present of a central force and is orbiting around its center point in exact circles, will have a constant velocity $|\dot{\mathbf{r}}| = \text{const.}$ and a constant radius $|\mathbf{r}| = \text{const.}$. These are directly connected to each other, which is described by Kepler's third law

$$T^2 = \frac{4\pi^2}{GM} a^3. \quad [10] \quad (1)$$

In this formula G is the gravitational constant and M is the mass of the Earth. The product of both $GM = 3.986... \cdot 10^{14} \text{ m}^3/\text{s}^2$ [11] can be measured with a high precision through satellite observations. The time for a complete orbit T is given by the measured velocity and the (mean) distance $|\mathbf{r}|$ of the satellite. For the assumed circular orbit, the semi-major axis a equals the geometric distance from the center of the Earth to the satellite $a = |\mathbf{r}|$.

In order to get an estimate of the quality of the circular orbit approximation, an average numerical eccentricity value ϵ of LEO satellites is required. The eccentricity is then calculated in the following way

$$e = a \cdot \epsilon. \quad [12] \quad (2)$$

The information about the numerical eccentricity ϵ and the altitude of known satellites can be found in a TLE catalogue [7].

In Fig. 2 a histogram of the numerical eccentricities of LEO satellites is displayed. It is visible that most orbits are close to being circular and the numerical eccentricity decreases rapidly. Its median value is $\bar{\epsilon} = 2.81\text{e-}3$. In

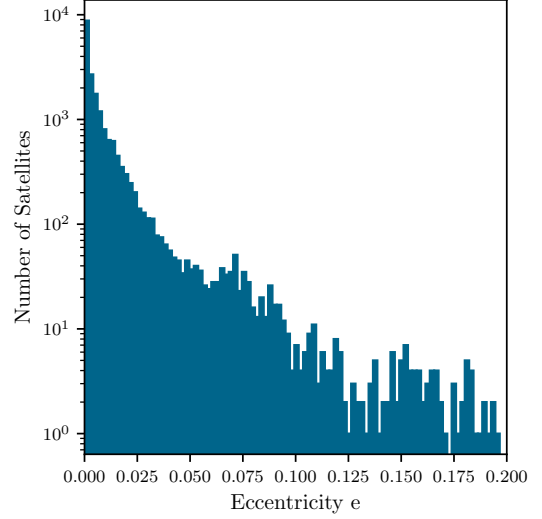


Figure 2. Logarithmic histogram of the eccentricity values of current satellites in LEO according to the Space Track catalogue [7].

order to convert ϵ into an uncertainty of the altitude measurement, two extreme cases have to be distinguished.

1. The RSO was measured at its perigee.
2. The RSO was measured at its apogee.

In the first case, the RSO was at its closest position. For the possible error in this case, the most distant position of the orbit, the apogee, must be considered. This is given by the following

$$h = a_1 - e_1 = a_1(1 - \epsilon) \Leftrightarrow a_1 = \frac{h}{1 - \epsilon} \quad (3)$$

$$\Rightarrow h_{\max} = a_1 + e_1 = a_1(1 + \epsilon) \Rightarrow h \frac{1 + \epsilon}{1 - \epsilon}, \quad (4)$$

where h is the measured altitude. It is also the point at which the RSO has its maximum possible distance h_{\max} considering the two cases. This applies analogously to the second case with a reversed sign. In this case the calculated distance to perigee is the closest point h_{\min} . The resulting error is as follows

$$\Delta h = h_{\max} - h_{\min} = h \frac{4\epsilon}{1 - \epsilon^2}. \quad (5)$$

The orbital altitude A examined in further calculations is $A = 700 \text{ km}$. With Eq. (5) and the determined mean value of the numerical eccentricity $\bar{\epsilon}$ the altitude error is $\Delta h = 79 \text{ km}$.

3. THEORETICAL CALCULATION

The goal of this work is to improve the error resulting for the circular orbit estimation and actually measure the altitude of the satellite. This is done by detecting the RSO using multiple APPARILLOs, while each of them measures the RA (right ascension) and Dec (declination) coordinates. The accuracy of a single system Δp by means of the streak detection and astrometry is set to be $\Delta p = 3$ px. This means that the RSO is captured at an angle equivalent to those 3 pixels. The accuracy d_i of the used system can then be calculated using basic geometry, which leads to the following equation

$$d_i = A \frac{\Delta p \cdot (S_i/R_i)}{f}. \quad (6)$$

The sensor size is $S = 36.9 \times 36.9$ mm with a resolution of $R = 4096 \times 4096$ px. The focal length f of the used lens is $f = 200$ mm. For a satellite at an altitude of $A = 700$ km the projected along and cross track error would be around $d = 95$ m. Based on the results of earlier work [6], this is a conservatively estimated value that will be achievable with the future system.

Each error can be visualised by a cone around the line of sight (LOS) which overlap at the RSO, see Fig. 3. To calculate the intersection volume two approximations

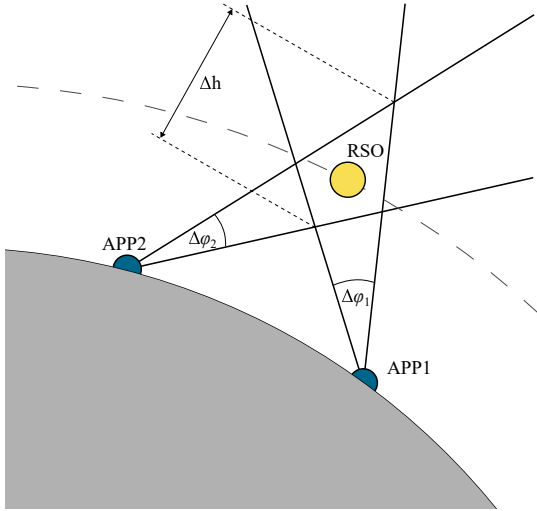


Figure 3. Two APPARILLOs detecting the same LEO object. The intersection of the error cones allows the altitude and its uncertainty to be specified.

were made.

- The first approximation is to neglect that the error cones diverge in the vicinity of the RSO. In mathematical terms, this means that the object becomes a cylinder. This approximation is justified, because the cone does not diverge that much at the relevant altitudes.

For example, the RSO is approximately at distance of 700 km and the FOV = $27.9''$. According to Eq. (6), this results in a diameter of $d = 95$ m. At an altitude of $(700 \pm d)$ km the difference of the diameter is $\Delta d = 3$ cm, which can be neglected.

- The second approximation is that the field of view of the three pixels responsible for the error is not a square. It is modified to be a circle. This means that the uncertainty of the satellite's position is the same in each direction of travel across the camera. This approximation is justified by the fact that the chosen uncertainty was derived from an average of previous work [6].

The two approximations are visualised in Fig. 4. This

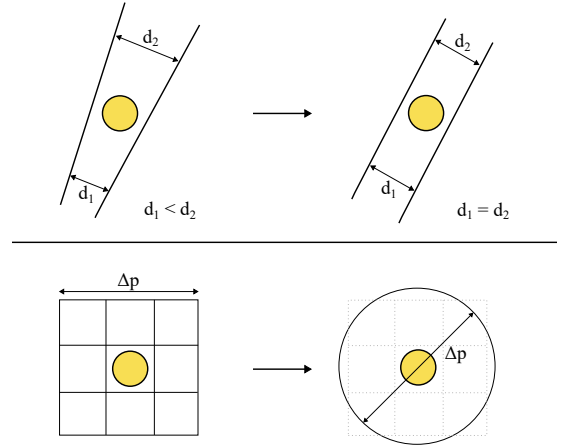


Figure 4. Visualisation of the approximations to calculate the intersection volume.

problem has now been simplified to a calculation of the intersection volume of two cylinders with an arbitrary angle α to each other. In this case and without restriction of generality it is possible to say that cylinder 1 is located around the z -axis. The center line of cylinder 2 is located in the zy plane in a way that both center lines will form the desired angle α . This results in the satellite being at $(0,0)$. For further calculations and to avoid mathematically undefined values it is also allowed to assume that the radius of the first cylinder R_1 is less than or equal to the radius of the second cylinder R_2 , $R_1 \leq R_2$. The hull C_i of a general cylinder can be given in the following way

$$C_i = \begin{pmatrix} R_i \cos(\varphi_i) \\ R_i \sin(\varphi_i) \\ z_i \end{pmatrix} \quad (7)$$

where R_i is the radius of the cylinder and $\varphi_i \in [0, 2\pi[$, $z_i \in \mathbb{R}$. This corresponds to the hull C_1 of cylinder 1 without further adjustments. The second cylinder is rotated around the x -axis with the chosen angle α and its boundary C_2 is then given by

$$C_2 = R_x(\alpha) \cdot C_1, \quad (8)$$

where $\mathbf{R}_x(\alpha)$ is the three-dimensional rotation matrix around the x-axis with an angle of α . The parameters of the resulting intersection curve

$$\mathbf{C}_1 = \mathbf{C}_2 \quad (9)$$

are calculated to be

$$R_2 \cos(\varphi_2) = R_1 \cos(\varphi_1) \quad (10)$$

and

$$z_1 = R_2 \sin(\varphi_2) \frac{1}{\sin(\alpha)} - R_1 \sin(\varphi_1) \frac{\cos(\alpha)}{\sin(\alpha)} \quad (11)$$

$$z_2 = R_2 \sin(\varphi_2) \frac{\cos(\alpha)}{\sin(\alpha)} - R_1 \sin(\varphi_1) \frac{1}{\sin(\alpha)}. \quad (12)$$

If these parameters are inserted into the original cylinder equations Eq. (7), two intersection curves $\mathbf{I}_{1/2}$ are obtained as a result. These curves are the edges of the resulting volume. In Fig. 5 an example result is displayed. Because the curvature of the surface area is always zero

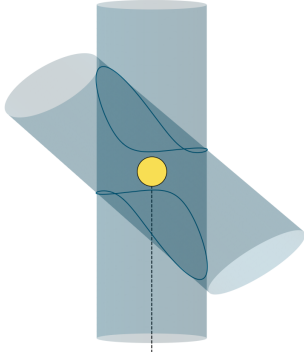


Figure 5. Intersection of the two error cones with an angle of $\alpha = 45^\circ$ while observing an RSO (yellow dot). The blue lines are the intersection curves and the dashed black line is the ground vector \mathbf{g} .

in one direction, only the edges are necessary to calculate the altitude difference. This can be visualised by placing such an object on a flat surface, like a table. In this case at least one edge of it always touches the table. To get the correct value for the altitude difference the correct ground vector \mathbf{g}' has to be found in the rotated coordinate system. With the knowledge of the rotations necessary to map both line of sights \mathbf{LOS}_1 , \mathbf{LOS}_2 to the desired constraints, the original ground vector \mathbf{g} can be then rotated accordingly. The result of the dot product of the modified ground vector \mathbf{g}' with the intersection curve \mathbf{I}_1 is the spatial difference of this curve along this ground vector.

$$\Delta h_1 = \max(\mathbf{g}' \cdot \mathbf{I}_1) \quad (13)$$

The intersection figure is point symmetric around the RSO. This means, to get the total altitude difference Δh the altitude difference to one edge must be doubled.

$$\Delta h = 2 \Delta h_1. \quad (14)$$

4. RESULTS

The established theoretical framework can now be used to find an optimal solution for the setup of two APPARILLOs. Each system has a large set of variables. To keep this analysis in a manageable format some variables are restricted to realistic values. The camera is fixed, it has a resolution of $R = 4096 \times 4096$ px and the sensor size is $S = 36.9 \times 36.9$ mm. The lens has a focal length of 200 mm. The resulting angle subtended by each pixel is then $FOV = 9.3''$. The error is set to be 3 times the FOV of a single pixel. The RSO is in an orbit with an altitude of 700 km.

4.1. The optimal placement and alignment

In the first step the influence of the spacing between the two APPARILLOs is investigated. In addition to this distance, the observation angle is a key factor of the accuracy. The distance between the two APPARILLOs is determined by the position of the RSO, the earth surface, and the observation angle of each APPARILLO, see Fig. 6. The RSO will also be in the plane of the two APPARILLOs, which is perpendicular to the horizon of each APPARILLO.

With these restrictions, the altitude uncertainty can be

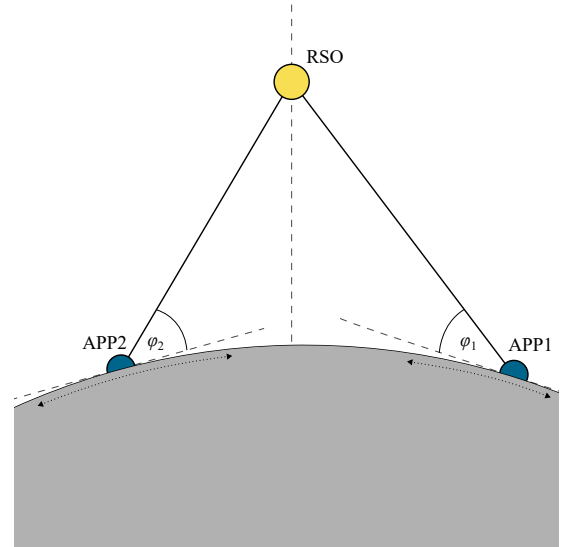


Figure 6. The position of an APPARILLO is determined by the observation angle φ_i . By varying this angle, the position of the APPARILLO shifts along the earth's surface.

calculated depending only on the two angles φ_1 and φ_2 . It is displayed in Fig. 7.

The results show values up to 500 m. Data above this limit is excluded, because the uncertainty is rising very fast and diverges in cases in which both APPARILLOs look in the same direction. This data would overshadow

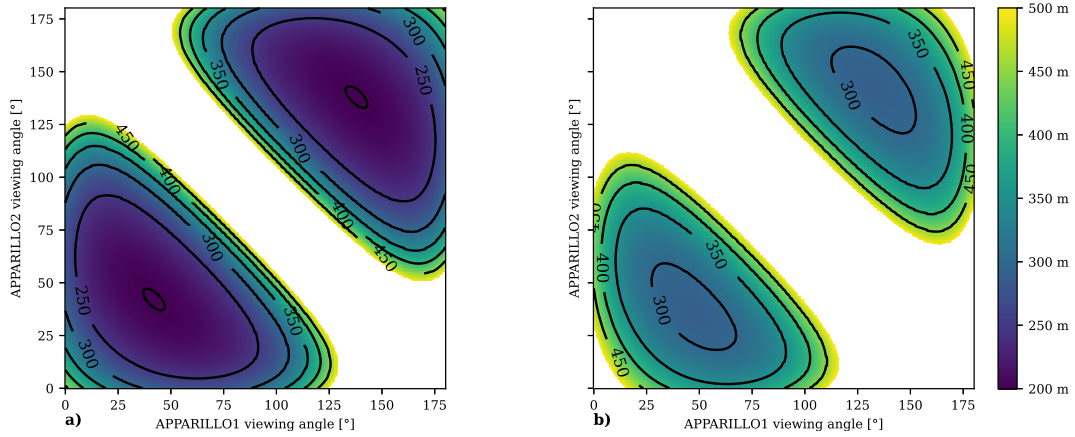


Figure 7. Result of the altitude uncertainty of measurements by two APPARILLOs in a bi-static observation condition. The two plots show different lens combination. In Figure a) both APPARILLOs have a 200 mm lens equipped. Figure b) shows the result when APPARILLO 1 has a 105 mm lens equipped.

the important features and is removed. For the selected hardware configuration, the optimal observation angle to achieve the lowest possible altitude uncertainty is 42° for both APPARILLOs. The triangulation is accurate up to 200 m and the best spacing of the two APPARILLOs is 1334 km along the surface of the earth.

The result is point symmetric around the $90^\circ, 90^\circ$ point, because the angle of one LOS with the ground vector has a symmetric extreme point at 90° . This situation describes the changing of the "observation sides", the APPARILLOs are mirrored and nothing changes in terms of content, compare Fig. 6. In addition to this it also has a symmetry axis that follows the line of origin. This is because both APPARILLOs have the same focal length and therefore the same uncertainty.

If the lens of APPARILLO 1 is changed to a smaller focal length $f = 105$ mm, Fig. 7 b), that system has a larger field of view, but also a larger error. The point symmetry is still present because the reason for it is only related to a single APPARILLO and the RSO. The second symmetry axis then no longer exists because the two APPARILLOs have different uncertainties and can not be exchanged anymore. The optimal spacing is longer at 1584 km and the RSO is closer to the APPARILLO 1, resulting in a steeper observation angle. The observation angles are $\varphi_1 = 46^\circ$ and $\varphi_2 = 36^\circ$. The smallest altitude uncertainty for this case is 289 m.

4.2. The fixed position

In this section a specific scenario is investigated. The position of both APPARILLOs is fixed at interesting locations. In this case, two APPARILLOs were placed in Stuttgart and in Andøya, the distance is about 2300 km. In contrast to the previous investigation, the position of the satellite RSO is now changed, but the altitude is kept constant at 700 km. The satellite can now also take positions that are not in the plane spanned by the two AP-

PARILLOs and the ground vector. This problem is also solved with the theory described in Section 3. The altitude uncertainty is shown in Fig. 8. The two blue dots mark the position of the APPARILLOs. The position of the satellite is projected onto its ground track and is given in latitude and longitude. The data that is on the imaginary connection line between the APPARILLOs is already contained in Fig. 7. It is symmetric around this axis. The best possible altitude uncertainty is 228 m. If the satellite moves between the two APPARILLOs in a corridor of 10° , the uncertainty remains below 250 m. It gets significantly worse when both observers are oriented in the same direction, for example, if both face south.

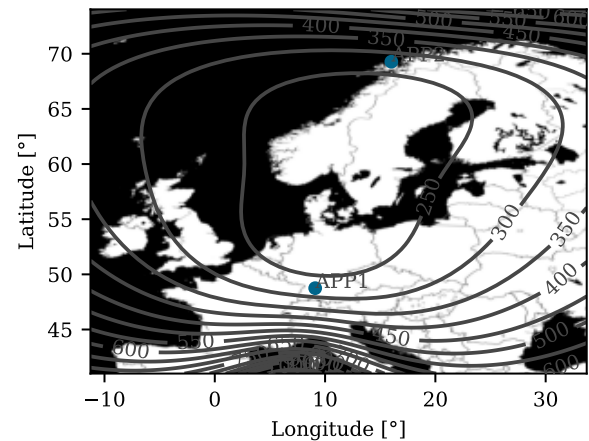


Figure 8. Altitude uncertainty map of a satellite observed by two APPARILLOs located in Stuttgart and Andøya. The displayed values correspond to the altitude uncertainty in meters. (Map tiles by Stamen Design, CC BY 3.0 — Map data © OpenStreetMap contributors)

5. COMPARISON AND SUMMARY

The results of the theory established in Section 3 show that it is possible to achieve altitude accuracies up to 200 m with only two APPARILLOs. The assumption that the object is on a circular orbit results in an uncertainty of 79 km. Compared to this assumption, the bistatic measurement would result in an error that is 2 orders of magnitude better. Besides the hardware choices, camera or lens, the location of both APPARILLOs is a key value to increase the accuracy. The optimal spacing between two APPARILLOs to detect objects at an altitude of 700 km is 1334 km, where both line of sights have an elevation of 42° . The theory also shows that this angle and accuracy is dependent on the used optics.

This work is the first step towards a network of multiple APPARILLOs. It determines guidelines to choose the distances between each APPARILLO and provides a theoretical framework to calculate the altitude uncertainty of measurements of a given configuration.

REFERENCES

1. Reising, C., et al. (2022). GESTRA - upgrading to future distributed phased array radar networks for space surveillance, In *Proc. IEEE International Symposium on Phased Array Systems and Technology*
2. Hampf, D. et al., (2018). Mini SLR: A fully automated miniature satellite laser ranging ground station. In *Proc. 69th International Astronautical Congress*
3. Wgner, P. & Clausen, T., (2022). APPARILLO: a fully operational and autonomous staring system for LEO debris detection. *CEAS Space Journal*, **14**, 303-326
4. Hampf, D., Sproll, F. & Hasenohr, T., (2017). OOOS: A hardware independent SLR control system. In *Proc. ILRS Technical Workshop*
5. Haussmann, R., Wagner, P. & Clausen, T., (2021). Streak detection of space debris by a passive optical sensor. In *Proc 8th European Conference on Space Debris*
6. Wagner P, (2022). *Ground-Based Autonomous Passive Optical Staring Sensor for Orbital Object Detection and Position Measurement*, Ph.D. thesis, Institute of Aerospace Thermodynamics (ITLR) University of Stuttgart
7. Space-Track. Full catalog 3LE. Online at <https://www.space-track.org/#recent>. (as of 1 December 2022)
8. Bernard, A., Nafi, A. M. & Geller, D., (2018). Using triangulation in optical orbit determination. In *Proc. AAS/AIAA Astrodynamics Specialist Conference*
9. Choi, J., Choi, Y.-J., Yim, H.-S., Jo, J. & Han, W., (2010). Two-Site optical observation and initial orbit determination for geostationary earth orbit satellites. *Journal of Astronomy and Space Sciences*, **27**, 337-343
10. Nolting, W., (2018). *Grundkurs Theoretische Physik 1*, Springer Spektrum Berlin, Heidelberg, ed. 11
11. Luzum, B., et al., (2011). The IAU 2009 system of astronomical constants: the report of the IAU working group on numerical standards for Fundamental Astronomy, *Celestial Mechanics and Dynamical Astronomy*, **110**, 293
12. Bronstein, I. N., Semendjajew, K. A., Musiol, G. and Muhlig, H., (2000). *Taschenbuch der Mathematik*, Harri Deutsch, ed. 5